NANO-SQUIDs based on niobium Dayem bridges for nanoscale applications

2010 J. Phys.: Conf. Ser. 234 042010

(http://iopscience.iop.org/1742-6596/234/4/042010)

Journal of Physics: Conference Series **234** (2010) 042010 doi:10.1088/1742-6596/234/4/042010

NANO-SQUIDs BASED ON NIOBIUM DAYEM BRIDGES FOR NANOSCALE APPLICATIONS

C. Granata, A. Vettoliere*, P. Walke*, E. Esposito, C. Nappi, P. Silvestrini°, B. Ruggiero, and M. Russo

Istituto di Cibernetica "E. Caianiello" del Consiglio Nazionale delle Ricerche, 80078 Pozzuoli (Napoli)-Italy

* Also Università degli Studi di Napoli "Federico II", Napoli-Italy

° Dipartimento di Ingegneria dell'Informazione, Seconda Università degli Studi di Napoli, Aversa(Caserta)-Italy

c.granata@cib.na.cnr.it

Abstract. We report on the design, the fabrication and the performance of an integrated magnetic nano-sensor based on niobium dc-SQUID (Superconducting QUantum Interference Device) for nanoscale applications is presented. The nano-sensors are based on nanometric niobium constrictions (Dayem bridges) inserted in a square loop having a side length of 200 nm. Measurements of voltage-flux characteristic, flux to voltage transfer factor and noise performances are reported. In small signal mode, the sensors have shown a magnetic flux noise spectral density of 1.5 $\mu\Phi_0/Hz^{1/2}$ corresponding to a spin sensitivity in unit of Bohr magneton of 60 spin/$Hz^{1/2}$. Supercurrent decay measurements of these devices are also reported. Such measurements provide useful information for applications which employ the SQUID as a trigger where the sensor works on the zero voltage state. The experimental data, have shown an intrinsic current fluctuation less than 0.2% of the critical current at liquid helium temperature, corresponding to an intrinsic sensor magnetic flux resolution of a few $m\Phi_0$. In view of the nano-SQUID employments in the detection of small spin populations, the authors calculated the spin sensitivity and the magnetic response relative to the single spin, as a function of its position within the SQUID hole. The results show that the SQUID response depends strongly on the spin position.

1. Introduction

In the last years, a stimulating challenge for the SQUID sensors is the detection of a single or a few electronic spins and the study of the magnetization reversal of nano-particles (nanomagnetism) [1-4]. Due to their insensitivity to background magnetic fields, such nano-SQUIDs are ideal for making local magnetic measurements. Reaching a spectral density of magnetic moment noise as low as few $\mu_B/Hz^{1/2}$ [5-8] (μ_B is the Bohr magneton) referred to a sensor geometrical area of about (200 x 200 nm2), the nano-SQUIDs are suitable for the above cited applications. Recently, preliminary measurements of magnetization from ferritin nano-particles have been reported [6].

In order to reach the suitable sensitivity, the SQUID loop dimension has to be as small as possible (100-200 nm), requiring Josephson junctions having deep sub-micron size. Due to the limits of the fabrication process, tunnel Josephson Junctions, can not be employed in such nano-SQUIDs. Dayem nano-bridges (nano-constriction of a superconducting film) fabricated by using Electron Beam Lithography (EBL) or Focused Ion Beam (FIB) represent a good alternative to the tunnel type junctions. So, a nano-SQUID consists typically of a niobium thin film ring (diameter of 100-400 nm) interrupted by two nano-bridges with a length and a width of less than one hundred of nanometers [5-8]. In the present paper, a detailed study of these devices is reported. In particular, in the second section the design, the fabrication and the main experimental performances (voltage-flux characteristics, flux-to-voltage transfer factor (responsivity) and noise properties) are reported. Preliminary experimental data concerning the critical current switching probability, which provide useful information about the intrinsic dissipation of such devices, are illustrated. In the third section, supercurrent decay measurements consisting of switching current distributions are reported. The fourth section is dedicated to a simulation study concerning the spin sensitivity and the magnetic response relative to the single spin (Bohr magneton), as a function of its position within the SQUID hole.

2. Sample fabrication and sensor performance

The device consists of a niobium loop interrupted by two bridges which constitute the lateral arms of the washer (Fig 1). This structure deviates from the typical washer loop, in particular the flux focusing effect is expected to be less effective. The side length of the square detection area (washer hole) is 200 nm while the length and width of the nano-bridge are 100 nm and 80 nm respectively. The superconducting loop has a washer shape in order to enhance the heat dissipation during the working operations when the sensor is current biased in resistive mode. The sample fabrication procedure has been described in details elsewhere [7], so only an outline of the sensor design and the main fabrication steps is given here. The fabrication process is based on thin films patterned by both electron beam lithography (EBL) and optical lithography as well as lift off and reactive ion etching (RIE) processes. Two integrated micrometric coils located close to the sensor allow an accurate magnetic flux calibration and an effective measurement of the voltage-flux characteristics. With respect to external coils they show a higher mutual inductance allowing to effectively measure the voltage-flux characteristics (V-Φ) and an easy flux biasing of the SQUID at the point corresponding to the maximum value of the flux to voltage transfer coefficient V_Φ (responsivity).

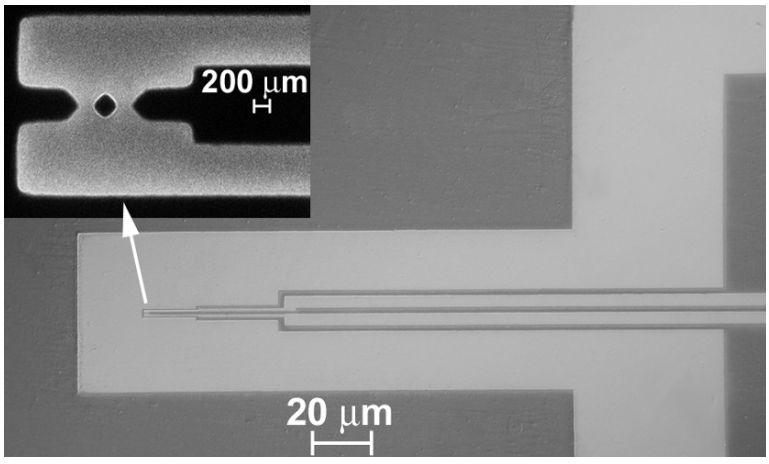

Figure 1. Scanning electron micrograph of an integrated nano-sensor including the micrometric integrated coil for the modulation/calibration operations. The inset shows the SQUID loop and the nanobridge Josephson junctions.

The measurements were performed in a liquid helium transport dewar. The devices were shielded by a lead/cryoperm coaxial double can. The read-out electronic for the measurements of both voltage-flux characteristics and noise performances is integrated on a very-low-noise miniaturized detection circuit having radio frequency filters on the electrical connections to room temperature. In Fig. 3 voltage–magnetic flux characteristics of a nano-SQUID having hysteresis free I-V characteristics, is reported. It was measured by feeding the closest integrated coil with an ac triangular current signal (10 Hz) of about 100 mA peak-to-peak by a standard waveform signal generator. Due to the integrated coils, it has been possible to measure up to three flux quanta. Note that the voltage-flux characteristics are a useful diagnostic tool to check the quality of the device, so the possibility of measuring the whole characteristics and accurately choosing the best operation flux bias represents an important sensor improvement. A voltage swing as high as 75 μV can be estimated from the experimental curve. Measuring the dc current flowing in the coil for the drift of a flux quantum, a current-flux transfer factor I_Φ of 42 mA corresponding to a mutual inductance between the coil and the SQUID $M=\Phi_0/I_\Phi=49$ fH has been obtained. In Fig 5 the spectral density of the flux noise, measured in small signal mode, is reported. It has been obtained by dividing the measured spectral density of the voltage noise $S_V^{1/2}$ by V_Φ which corresponds to the dc magnetic flux bias during the voltage noise measurements. The best noise performance is typically obtained by biasing the SQUID at its maximum V_Φ value, which is detected by maximizing a small signal while both the bias current and the dc magnetic flux bias are varied. The sensor exhibits a magnetic flux noise level of 1.5 $\mu\Phi_0/Hz^{1/2}$ in the white region corresponding to a spin noise, in unit of Bohr magneton, of $S_n^{1/2}=2aS_\Phi^{1/2}/(\mu_B\mu_0)\sim100$ spin/$Hz^{1/2}$ where a is the radius of the SQUID loop, μ_0 is the magnetic vacuum permeability and $\mu_B = 9.27 \times 10^{-24}$ A m^2. However the above formula is based on a pessimistic assumption for the coupling, if an optimal one is taken into account a spin sensitivity value as low as 20 spin/$Hz^{1/2}$ is obtained. This value is comparable with the best value reported in the literature [6]. In the inset of Fig. 2b the flux-to-voltage transfer factor as a function of the applied magnetic flux is reported. It has been obtained by taking the derivative of the V-Φ curve in the range from Φ=0 to $\Phi=\Phi_0/2$. A maximum V_Φ value as high as 1.6 mV/Φ_0 for an applied flux of about 0.2 Φ_0 can be evaluated from the curve. The asymmetry of the curve with respect to the maximum is due to the different curve slopes of the V-Φ characteristic in proximity of the minimum and maximum. The high responsivity is due to the large values of both critical current modulation depth and the dynamical resistance Rd close to the zero voltage state (20 Ω). A high value of V_Φ reduces the amplifier noise contribution to a tolerable level.

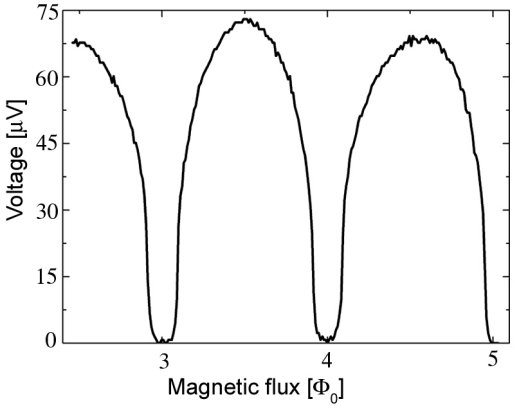

Fig.2a. Voltage-magnetic flux characteristics of a nano-device. Note that the V-F characteristics are resonances-free and smooth, allowing the sensors to operate in a wide range of bias points.

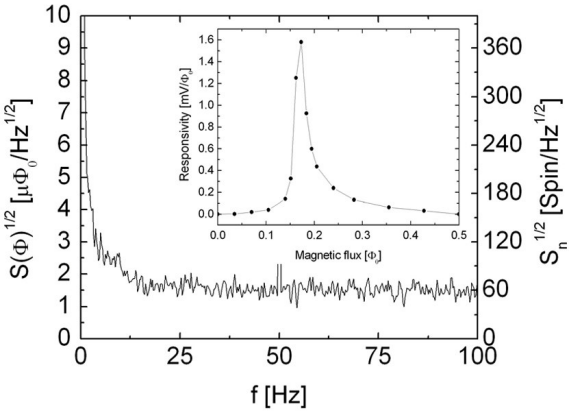

Fig.2b. Nano-sensor magnetic flux spectral density measured in the small signal mode, using a low-noise readout electronics. The inset shows the responsivity as a function of applied magnetic flux.

3. Supercurrent decay measurements

The switching current distribution measurements provide useful information for applications which employ the SQUID as a trigger (cold mode) where the sensor works on the zero voltage state [9]. In fact it is possible to evaluate the intrinsic magnetic flux resolution of a nano-SQUID working in the trigger mode. In the cold mode operation, the SQUID shows a hysteretic characteristic and it is current biased close the critical current; the magnetization reversal of a particle triggers the transition of the SQUID to the normal state. In the Fig. 3a is reported the current-voltage characteristic at T=4.2 K of a nano-SQUID including two nano-bridges with a length and width are 280 nm and 120 nm respectively. As expected the sensor shows an evident hysteresis due to the greater nano-Bridge size. The Fig. 3b shows the experimental dependence of the switching current distributions from the zero voltage state P(I) and the related escape rates Γ, as a function of the bias current I, at different temperatures measured using the standard fly technique [4,10] Theoretical curves are obtained using the thermal theory in the moderately damping limit. The fitting parameters are C=1 fF, I_{c0}=506 μA, R=50 Ω, $Q=\omega_p RC=2$ and T=4.2 K. As it is evident in Fig 3, the theoretical predictions are in good agreement with the experimental data indicating that the escape process from the metastable state in these devices can be reasonably described in the framework of a thermal theory in the moderately damping limit (Q≥1) [11]. The supercurrent decay measurements have been used to evaluate the intrinsic magnetic flux resolution of the sensor working in the cold mode. We can define a magnetic flux resolution ΔΦ as the minimum external magnetic flux required to yields a switching from the metastable zero voltage state to the normal state. ΔΦ is related to the current-to-flux transfer factor (current responsivity) ∂Ic/∂Φ and to the switching current distribution width σ:

$$\Delta\Phi = \frac{\sigma}{2\dfrac{\partial I_c}{\partial \Phi}} \qquad \sigma = \sqrt{\langle I^2\rangle - \langle I\rangle^2} \tag{1}$$

by using a current responsivity value of 200 μA/Φ_0 measured at a maximum slope point of the I_c-Φ_e characteristic, and the experimental s obtained from the experimental data of fig 3b, it is possible to evaluate an intrinsic magnetic flux resolution of about 2 mΦ_0.

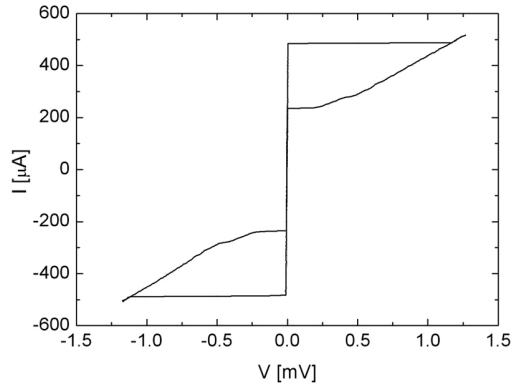

Figure 3a. dc Current-voltage characteristic of a hysteretic nano-SQUID measured a T=4.2 K. The sensor shows a critical current Ic of about 500 mA and an evident hysteresis.

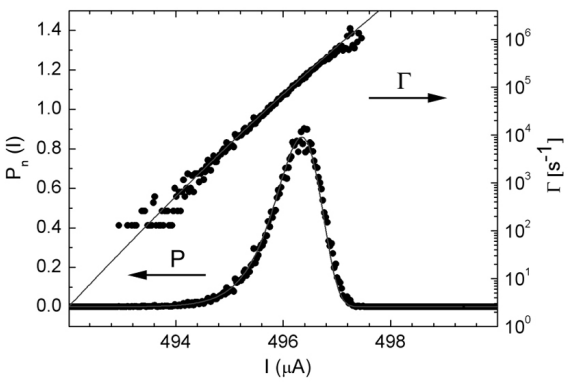

Figure 3b. Experimental data (dots) and theoretical predictions in the moderately damping limit (solid lines) of the switching current distribution (P) and the escape rates (G) vs the bias current I of a nanoSQUID measured at T=4.2K.

4. Spin sensitivity simulations

In view of the nanomagnetism applications of the nano-SQUIDs, a study of the magnetic coupling between the nano-objects or spins and the SQUID is very useful [12,13].

Here, the magnetic flux output and the spin sensitivity of the nano-SQUID are computed for a Bohr magneton (single spin) as a function of the position within the loop. We have considered a square geometry as the best approximation of the real situation and we have also supposed that the magnetic moment is oriented along the z-axis and its distance from the coil's plane is much smaller than a, at least of a ratio z'/a =0.05, so that the particle can be reasonably considered in the plane of the loop and no field divergence arises in correspondence of the loop edges. The components of the magnetic vector potential **A(r)** at position **r**(x,y,z), relative to a Bohr magneton oriented along the z-direction and positioned in (x',y'z'), are:

$$A_x = -\frac{\mu_0 \mu_B}{4\pi}\frac{(y-y')}{r^3}; \qquad A_y = -\frac{\mu_0 \mu_B}{4\pi}\frac{(x-x')}{r^3} \tag{2}$$

Here μ_0 is the magnetic vacuum permeability, and $\mathbf{r} = [(x-x')^2+(y-y')^2+(z-z')^2]^{1/2}$. The magnetic flux threading the loop is:

$$\Phi(x',y',z') = \oint \vec{A}\cdot d\vec{s} \tag{3}$$

where the integral is considered along the closed line of the SQUID loop. The integral (3), which could be analytically expressed, provides the magnetic flux threading the loop produced by a single spin as a function of its position within the loop [14].

A relevant figure of merit of a nano-SQUID for the detection of small spin populations is the spin sensitivity or spectral density of the spin noise $S_n^{1/2}$(the minimum detectable spin number per band unit). Using the expression of magnetic flux due to the single spin (obtained using resolving the equation 3) and the spectral density of the flux noise $S_\Phi^{1/2}$, it is possible to obtain $S_n^{1/2}$ as a function of the spin position within the loop.

$$S_n^{1/2}(x',y',z') = \frac{S_\Phi^{1/2}}{\Phi(x',y',z')} \tag{4}$$

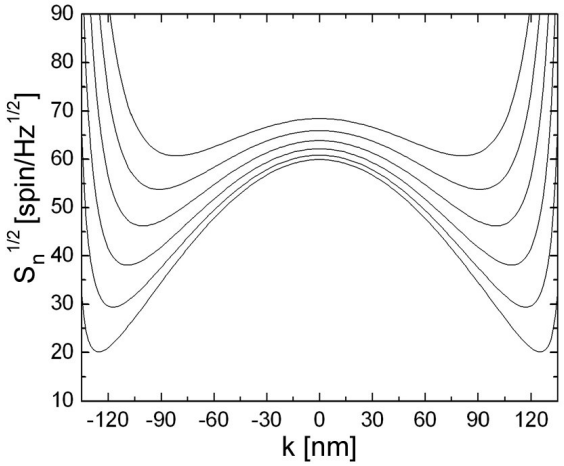

Figure 4a. Spin noise spectral density $S_n^{1/2}$ of a square nanoSQUID as a function of the position within its loop computed along a diagonal of the sensor loop for different z values.

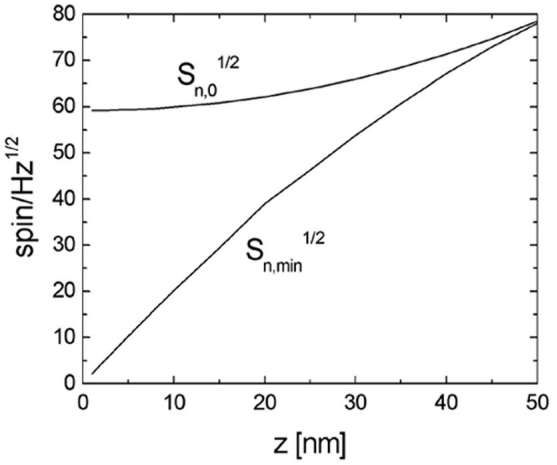

Figure 4b. Behaviors of the sensitivities $S_{n,min}^{1/2}$ and $S_{n,0}^{1/2}$ as a function of the distance z', evaluated at its minimum and at the center's sensor respectively

Fig. 4a reports the spin noise spectral density $S_n^{1/2}$ of a square nanoSQUID as a function of the position within its loop computed along a diagonal of the sensor loop, computed for different z values ranging from 10 nm to 35 nm. The lowest curve refers to z=10 nm, the highest to z=35 nm The setting parameters are a loop side length a=200 nm and a flux noise $S_\Phi^{1/2} = 1.5\ \mu\Phi_0/Hz^{1/2}$. In Fig. 4b, the sensitivities $S_{n,min}^{1/2}$ and $S_{n,0}^{1/2}$ as a function of the distance z', evaluated at its minimum and at the center's sensor respectively, are reported. $S_{n,min}^{1/2}$ value varies of about two magnitude orders in a z'-range of 50 nm, while $S_{n,0}^{1/2}$ only of a 20%. Note that for a large spin distance from the sensor plane, the spin sensitivities tend to the same value, indicating that they do not depend any longer on the spin position within the loop sensor.

5. Conclusions

A high spin sensitivity nano-SQUID based on niobium nano-bridges has been presented. Beside the standard SQUID characterization (voltage-flux characteristics, responsivity, flux and spin noise), interesting measurement of the supercurrent decay aimed to evaluate the intrinsic flux resolution are also reported. On the basis of a theoretical study concerning the calculations of the flux and the spin sensitivity of the nano-sensor as a function of the spin position within its loop, it comes out that the sensor performance strongly depends on the nano-object position reaching a ratio between the minimum and the maximum value of the sensor sensitivity of about 3 . Due to the recent successful efforts devoted to finely arrange the nano-particles within the sensor loop, the information here provided are very useful to optimize the sensor performance in view of most nano-magnetism applications.

References

[1] W. Wernsdorfer, Superc. Sci. Technol., 22 064013 (2009).
[2] C. P. Foley and H. Hilgenkamp, Superc. Sci. Technol., 22 064001 (2009).
[3] P. F. Vohralik and S. K. H. Lam, Superc. Sci. Technol., 22 064007 (2009).
[4] C. Granata, A. Vettoliere, R. Russo, E. Esposito, M. Russo and B. Ruggiero Appl. Phys. Lett., 94 062503 (2009).
[5] A. Vettoliere, C. Granata, E. Esposito, R. Russo, L. Petti, B. Ruggiero, and M. Russo, IEEE Trans. Appl. Supercond. 19, 702 (2009).
[6] L. Hao, J. C. Macfarlane, J.C. Gallop, D. Cox, J. Beyer, D. Drung, and T. Schurig, Appl. Phys. Lett., 92, 192507 (2008).
[7] C. Granata, E. Esposito, A. Vettoliere, L. Petti, and M. Russo Nanotechnology, 19, 275501 (2008).
[8] A.G.P. Troeman, H. Derking, B. Borger, G. Pleikies, B. Veldhuis and H. Hilgenkamp, Nano Lett., 7, 2156 (2007).
[9] W. Wernsdorfer, D. Mailly and A. Benoit J. Appl. Phys. 87, 5094 (2000).
[10] B.Ruggiero, C. Granata, V.G. Palmieri, A. Esposito, M. Russo, and P. Silvestrini, Phys. Rev. B 57 137, (1998).
[11] H. Grabert, P. Olschowski, and U. Weiss, Phys. Rev. B 36, 1931 (1987).
[12] D. L. Tilbrook, Superc. Sci. Technol., 22 064003 (2009).
[13] V. Bouchiat, Superc. Sci. Technol., 22 064002 (2009).
[14] C. Granata, A. Vettoliere, P. Walke, C. Nappi and M. Russo, J. Appl. Phys., 106, 1 (2009)